Turbulent flows at cryogenic temperatures: a new frontier

1999 J. Phys.: Condens. Matter 11 7761

(http://iopscience.iop.org/0953-8984/11/40/308)

J. Phys.: Condens. Matter **11** (1999) 7761–7781. Printed in the UK PII: S0953-8984(99)05393-X

Turbulent flows at cryogenic temperatures: a new frontier

L Skrbek, J J Niemela and R J Donnelly

Cryogenic Helium Turbulence Laboratory, Department of Physics, University of Oregon, Eugene, OR 97403-1274, USA

Received 22 June 1999, in final form 27 July 1999

Abstract. Cryogenic helium is of significant value in generating, and studying, the highest possible Reynolds and Rayleigh number flows under controlled laboratory conditions, primarily due to its extremely low value of kinematic viscosity. We consider here critical helium gas and the two liquid phases, helium I and helium II. Such flows are already being generated and studied using suitable cryogenic equipment. We outline the current experiments and existing proposals for future studies that include gaseous and liquid helium I and II.

1. Introduction

Turbulent flows occur commonly in nature and play an essential role on all scales, from galactic formation to the circulation of blood within our bodies. Measures of turbulent intensity are given by the Reynolds number

$$Re = \frac{UL}{\nu} \tag{1}$$

for essentially isothermal flows with characteristic length scale L and velocity U, and the Rayleigh number

$$Ra = \frac{g\alpha\Delta T L^3}{\nu\kappa} \tag{2}$$

for thermally driven flows in a gravitational field g, where ν, α and κ are respectively the kinematic viscosity, thermal expansion coefficient and thermal diffusivity, and ΔT is the temperature difference in the direction of g.

To appreciate the order of magnitude of these dimensionless numbers that characterize different kinds of turbulent flow in nature and engineering, we give some examples in table 1. Note that most natural turbulent phenomena occur on large scales L and are characterized by large values of these numbers.

It is well known that despite a long period of intensive research a general theory of turbulence is still lacking and computer simulations based on the Navier–Stokes equation are limited to moderate Re numbers of the order of several hundred. Since controlled laboratory experiments are constrained in L, it is desirable to study such situations using a working fluid possessing the smallest possible ν.

Helium offers three cryogenic fluids of interest (see figure 1). The first is critical helium gas, a heavy gas of helium near the critical point whose temperature is 5.20 K (on the ITS-90 scale) and whose pressure is 2.26 atm. Dynamically it is a classical fluid, but has properties strongly dependent upon the temperature and pressure.

0953-8984/99/407761+21$30.00

Table 1. Some examples of high Reynolds and Rayleigh number flows.

Example	*Ra*	*Re*
Sun	$\approx 10^{21}$	$\approx 10^{13}$
Ocean[a]	$\approx 10^{20}$	$\approx 10^{9}$
Atmosphere	$\approx 10^{17}$	$\approx 10^{9}$
Naval applications[b]		$\approx 10^{9}$
Aerospace applications[c]		$\approx 5 \times 10^{8}$

[a] $L \approx 1$ km, $\Delta T \approx 1\,^{\circ}$C.
[b] Length-based *Re* for submarine (SSN688).
[c] *Re* based on fuselage of Boeing 747.

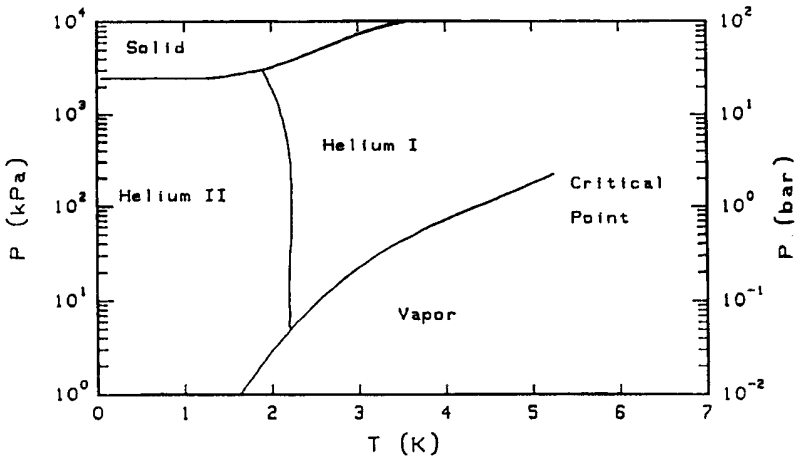

Figure 1. The phase diagram of liquid and gaseous helium.

Along the saturated vapour line we can identify two liquid phases of helium. Helium I has its normal boiling point at 4.2 K and exists at down to the lambda transition at 2.1768 K (again on ITS-90) at the saturated vapour pressure. It is a Navier–Stokes fluid. For temperatures below the lambda point, a new liquid phase forms which is called helium II, and which exhibits superfluidity. It remains a liquid at absolute zero of temperature; indeed, a pressure of about 25 bar is needed to solidify it.

Helium is by now probably the most studied and measured substance, exceeding our knowledge even of water. This means that the Reynolds and Rayleigh numbers and other derived quantities that depend on them are likely to be quite reliable. For properties of liquid helium at the saturated vapour pressure, see Donnelly and Barenghi (1998).

It is important to point out that helium is not only the fluid of lowest viscosity (see figure 2), it is able to reach a number of remarkable extremes in various ways. For example, in thermal convection using critical helium gas the Rayleigh number can be extremely large due to the ratio of fluid properties $\alpha/\nu\kappa$ appearing in it, which is some ten million times larger than for water (see table 2).

Helium also offers a great deal of flexibility. The properties of air used in a wind tunnel or of water used in a flow facility cannot, as a matter of practical interest, be changed by much if operating under ambient conditions. With helium, however, the properties can be changed over a wide range by changing the pressure and temperature. For helium gas, the properties vary rapidly with temperature, and especially with pressure. Properties of liquid helium I vary

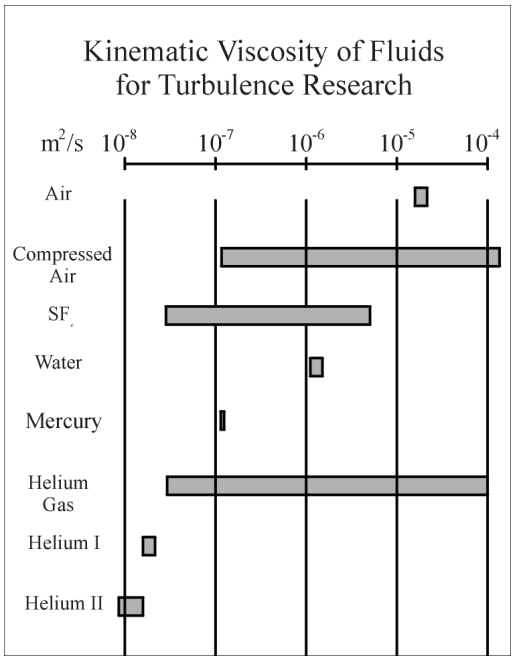

Figure 2. Extremes of accessible kinematic viscosity of different fluids. For air the usual situation is near 20 °C and 1 bar; for compressed air, the highest kinematic viscosity corresponds to 300 K, 0.1 bar, and the lowest to 300 K, 180 bar. For water the usual situation is 20 °C, 1 bar, similarly for mercury. For SF_6 the highest kinematic viscosity corresponds to 300 K, 0.5 bar and the lowest to 300 K, 50 bar. For helium gas the highest kinematic viscosity corresponds to 300 K, 0.1 bar, and the lowest to 6 K, 4 bar. For helium I the highest kinematic viscosity is at 4.2 K and SVP, the lowest is for saturated vapour pressure (SVP) at 2.2 K. For helium II, the highest kinematic viscosity (based on the total density) is at 2.15 K, SVP and the lowest at 1.7 K, SVP.

Table 2. Fluid parameters for various fluids used in turbulence research.

Fluid	T (press.)	ν (cm^2 s^{-1})	ρ (g cm^{-3})	α (K^{-1})	κ (cm^2 s^{-1})	$\alpha/\nu\kappa$
Air	20 °C	0.150	1.21×10^{-3}	3.67×10^{-3}	0.200	0.122
Water	20 °C	1.004×10^{-2}	0.998	2.07×10^{-4}	1.43×10^{-3}	14.4
SF_6	50 °C (50 bar)	2.8×10^{-4}	1.07	4×10^{-2}	1.9×10^{-4}	7.5×10^{5}
Mercury	20 °C (SVP)	1.14×10^{-3}	13.55	1.81×10^{-4}	4.63×10^{-2}	3.43
Helium I	2.25 K (SVP)	1.96×10^{-4}	0.146	0.0204	3.2×10^{-4}	3.25×10^{5}
Helium II	1.8 K (SVP)	9.01×10^{-5}	0.145	—	—	—
Helium gas	5.5 K (2.8 bar)	3.21×10^{-4}	0.0685	2.86	6.31×10^{-5}	1.41×10^{8}

significantly with temperature, even at the saturated vapour pressure. This fact allows liquid helium to be used to great advantage in free surface modelling of ships, as will be discussed in section 5 below.

While liquid and gaseous helium have many advantages, there are also disadvantages; not the least among them is the necessity for some knowledge of cryogenic engineering in order to properly design an experiment. Of course, other fluids can be used for reaching highly turbulent conditions by operating in the vicinity of their critical points. For example, heavy gases such as SF_6 are useful for convection research, as can be appreciated in the recent theses by Belmonte (1994) and Ashkenazi (1997), but also have their own disadvantages, such as

operation at high pressures. A recent summary of the subject of fluid properties at critical points is given by Belmonte (1994) and Maddocks (1998), who concludes from a comparison of helium, nitrogen, SF_6, air and water that the highest Reynolds and Rayleigh numbers will be achieved with helium.

There are other advantages to helium as well. One is ease of temperature control and associated thermometry, which have been developed to a very high degree of accuracy (Lipa 1998). Another is the reduction of noise owing to the low temperature. A third is access to superconducting technology, such as SQUIDs and superconducting magnetic suspension and balance systems (Britcher 1998).

There are a number of experiments one can do with cryogenic helium as well as novel devices that can be developed to take advantage of either the cryogenic environment or the properties of low temperature helium. A tentative list includes thermal convection using supercritical helium gas, high Reynolds number pipe flow, flow tunnels for generation of high Reynolds numbers for basic research and for testing models, tow tanks for wave generation experiments and for testing surface vessels, various grid flows and Taylor–Couette experiments.

In this paper, we discuss aspects of the current state of the cryogenic helium turbulence research and describe some experiments currently in progress. We also outline some likely future development of this interdisciplinary field that combines cryogenics with fluid dynamics and turbulence research, low temperature physics and materials research. We start with thermal turbulence in critical helium gas and then discuss various isothermal flows that are traditionally described by the Navier–Stokes equations.

Thanks to the demand for large scale refrigeration for superconducting magnets in high energy physics, the facilities to use helium in large scale experiments are already at hand in a number of nuclear and high energy laboratories both in the United States and abroad (Quack 1998).

2. Turbulent thermal convection experiment

Rayleigh–Bénard convection occurs in a horizontal layer of fluid of thickness L confined between perfectly conducting top and bottom surfaces. The bottom surface is heated and the top cooled in such a way that a steady temperature difference ΔT is maintained between the surfaces. In the so-called Boussinesq approximation (see, for example, Tritton 1988) the equations of motion read

$$\left(\frac{\partial}{\partial t} - \kappa\nabla^2\right)T = -\boldsymbol{u}\cdot\boldsymbol{\nabla}T \tag{3}$$

$$\left(\frac{\partial}{\partial t} - \nu\nabla^2\right)\boldsymbol{u} = -\boldsymbol{u}\nabla\boldsymbol{u} - \frac{1}{\rho}\nabla P + \boldsymbol{n}\alpha g T \tag{4}$$

$$\nabla\boldsymbol{u} = 0 \tag{5}$$

where P is the pressure, ρ the mean density and $\boldsymbol{u}$ the velocity vector. In the Boussinesq approximation variations of all fluid properties other than the density are ignored completely. Variations of the density are ignored except insofar as they give rise to a gravitational force. From the dimensional analysis of equations (3)–(5) it follows that the description of the thermal convection depends upon two dimensionless parameters, the Rayleigh number defined above and on the Prandtl number

$$Pr = \nu/\kappa. \tag{6}$$

In particular, the convective heat transfer, H, can be expressed by the Nusselt number

$$Nu = \frac{H}{H_0} = f\,(Ra, Pr) \tag{7}$$

where $H_0 = \kappa \Delta T/L$ is the heat transport due to conduction only. The functional dependence (7) depends on boundary conditions, in particular on the aspect ratio $\Gamma = D/L$, where D is the horizontal size of the convection cell. Thermal convection has been extensively studied both theoretically and experimentally, using various working fluids, such as water, air, mercury, SF_6 etc. Depending on the geometry (aspect ratio), heat is typically transferred by conduction alone for $Ra < 2000$, i.e, $Nu = 1$. For higher Ra there are successive regions of steady convection, oscillatory convection, chaos, transition to turbulence and regions sometimes called soft and hard turbulence that are identified by power-law scaling relations $Nu \propto Ra^m$ (assuming Pr stays approximately fixed). Of particular interest (for application in astrophysics, geophysics, oceanography, meteorology etc) is an asymptotic form of this scaling law for very high Ra.

It has been known for many years that there are some advantages in conducting thermal convection experiments at cryogenic temperatures. There are also disadvantages, one of which is that visualizing the helium flow under cryogenic conditions is both conceptually and technically more difficult, although some progress has been reported by Woodcraft *et al* (1998).

The first thorough study of thermal convection in helium I was due to Ahlers (1972), Ahlers and Graebner (1972) and Ahlers (1974). Our group has also reported on experiments in helium I (Niemela and Donnelly 1991).

While working on a somewhat unrelated matter, Pippard (1998) came to realize the potential of critical helium gas for a Rayleigh–Bénard experiment. His student Threlfall (1975) used a small cylindrical cell with aspect ratio $D/L = 2.5$ ($D = 48.4$ mm) and investigated a range of Ra from 60 up to 2×10^9. From the upper four decades of Ra he obtained the scaling relation $Nu \propto Ra^\gamma \cong 0.173 Ra^{0.28}$.

This research was continued and extended by Libchaber's group in Chicago. Sano *et al* (1989), Wu and Libchaber (1991) and Wu (1991) reported results on Rayleigh–Bénard experiments with cylindrical experimental cells of aspect ratio 0.5, 1 and 6.7 for Ra up to 10^{14}. They observed large-scale coherent flow, and from the temperature fluctuation spectra were able to distinguish a transition between so-called 'soft' and 'hard' turbulence. The transition between those two regimes was reported to be around $Ra \approx 10^8$, but the scaling relation between Nu and Ra did not appreciably change. They found that for Ra above about 10^8 Nu scales with Ra with power close to $\gamma \cong 2/7$.

Rayleigh–Bénard experiments using critical helium gas have been continued in Grenoble (Chavanne *et al* 1996, 1997). The experiments have explored the range of Ra from 10^3 to above 10^{14}, using a cylindrical cell with aspect ratio $\Gamma = 0.5$ ($L = 20$ cm). In contrast to the Chicago experiments, an increase in the scaling exponent was observed. These authors claim that for $Ra > 10^{11}$ they may have observed a transition to a fully turbulent asymptotic regime characterized by the scaling exponent $\gamma = 1/2$ predicted by Kraichnan (1962).

From the theoretical standpoint the question about *Nu–Ra* scaling for fully developed turbulence can be still regarded as an open one, despite a number of theoretical works on this subject. Siggia (1994) recently wrote a comprehensive review on existing theories. Here, we consider only a few important ideas.

The heat transport in the turbulent thermal convection is usually viewed as consisting of heat flow through some kind of thermal boundary layer occurring next to the top and bottom plates and through a turbulent core. A marginal stability theory (Malkus 1963) assumes two well defined thermal boundary layers of thickness λ, where the heat is transported by conduction and is responsible for the entire temperature drop. The assumption is that the thickness of the boundary layer adjusts itself to be marginally stable, with $Ra = Ra_c$, the

critical value for the onset of convection (Chandrasekhar 1961). By analogy with (2) we can write $Ra_c = g\alpha\lambda^3\Delta T/2\nu\kappa$, since half the temperature drop occurs over each boundary layer. Assuming that the heat is transferred through each boundary layer by conduction, i.e., $\dot{Q} \propto 1/\lambda$, the Nusselt number must scale as $Nu \propto Ra^{1/3}$.

However, there is ample experimental evidence that the scaling power is smaller than $1/3$ and that this simple picture does not hold. Indeed, a mixing length theory (Castaing *et al* 1989), motivated by experiments of the Chicago group, predicts a scaling law $Nu \propto Ra^{\gamma}$ with $\gamma = 2/7$. In this theory, three layers are assumed for the convecting fluid: a mixed inner core, a conventional thermal boundary layer and an intermediate plume-dominated layer. In a different manner, Shraiman and Siggia (1990) also obtained the same scaling exponent by introducing a viscous sublayer and a turbulent boundary layer. It is clear, however, that more work is needed to clarify the role of the thermal and velocity boundary layer thickness; i.e., the dependence of the scaling law due to Prandtl number. For critical helium gas with Pr of the order of unity, it can be estimated that the thickness of the thermal and velocity boundary layers would match at around $Ra \approx 10^{16}$.

Clearly, there is a need for experiments in which higher Ra can be achieved. Therefore a much larger cell, 1 m high and 0.5 m in diameter, was designed and constructed (see figure 4). It is situated in the Cryogenic Helium Turbulence Laboratory at the University of Oregon and a first experiment has provided valuable data on turbulent Rayleigh–Bénard convection with critical helium gas (4.3 K $< T <$ 6 K, 0.1 mbar $< P <$ 3 bar) as a working fluid (Niemela *et al* 1999). This apparatus has the capability to span up to ten orders of magnitude of the control parameter, Ra (up to 10^{16}), the highest Ra ever reached in the laboratory. Such a large range of Ra in a single experiment is achieved by changing the density and mean temperature of the working fluid together with the temperature difference between the lower and upper copper plates. Preliminary experiments which take into account corrections to the adiabatic temperature gradient show no signs of any transition into the predicted ultimate *Nu–Ra* scaling, at least up to $Ra = 2 \times 10^{15}$.

At this point it is important to point out that the gas properties used to determine Nu and Ra were obtained using commercial software incorporating the most recent *NIST Standard Reference Database* 12 adopted in 1992, but modified for increased accuracy near the critical point (Arp and McCarty 1998). Changes in the accepted values of the fluid properties between NIST 12 and the older *NBS Technical Note* 631 (McCarty 1972) values used by Wu (1991) have some effect on the scaling properties of the Nusselt number.

We should emphasize that our cell, because of its size, is best suited for reaching high Ra data within the Boussinesq approximation, by using the working fluid away from the critical point. Furthermore, consistent with current knowledge, we believe our copper plates can be considered smooth (estimated surface roughness is better than 10 μm) and so possible changes in scaling due to surface roughness should not be an issue.

It is certainly very important to find out what happens above $Ra \approx 10^{16}$, where for the working fluid with Pr of the order of unity the thickness of the thermal and velocity boundary layer are predicted to match. Currently the experiment is being continued in order to reach Ra beyond this value.

In addition to global heat transfer studies, we use neutron transmutation doped semiconducting germanium sensors, in the form of 250 μm cubes with 1 mil brass leads attached to their opposite faces, to monitor the turbulent flow inside the cell. From the observed temperature fluctuations, we can calculate temperature power spectra. With increasing Ra, they gradually develop an inertial range displaying several orders of magnitude of Bolgiano-like $-7/5$ scaling (see, e.g. Monin and Yaglom 1975) as illustrated in figure 3 for the case $Ra = 1.3 \times 10^{14}$.

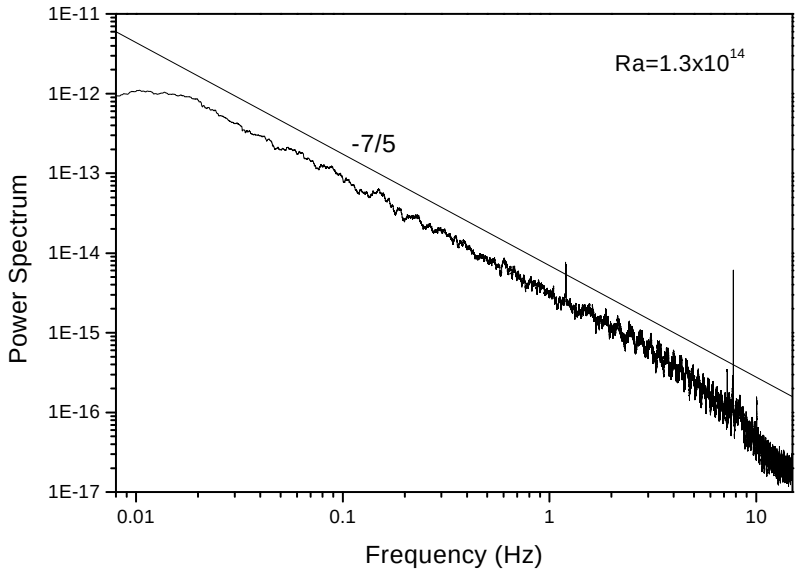

Figure 3. Temperature fluctuation spectrum obtained for $Ra = 1.3 \times 10^{14}$ showing Bolgiano-like scaling.

Although the Oregon cell is designed to reach the highest Ra, in a controlled laboratory experiment (under Boussinesq conditions) it is the prototype of a much larger experiment designed to study ultra-high Ra flows involved in large scale natural phenomena as outlined in table 1.

A conceptual design for a 10 m cell was presented some time ago (Donnelly 1994) and is shown in figure 5. Experience gained with the 1 m cell will be invaluable in designing the 10 m cell.

We propose to hold $D/L = 0.5$, retain T and ΔT between the plates to assure Boussinesq conditions. Under these conditions we can multiply the present value $L = 1$ m by a scaling factor s (Donnelly 1994). It is easy to see that since Ra increases as s^3, Nu should scale roughly linearly with s (exactly if the *Nu–Ra* scaling exponent were $1/3$). Thus the heat load scales roughly quadratically with s. Using our present data we can estimate the expected performance of the large cell: $Ra \cong 10^{19}$ should correspond to $Nu \cong 4 \times 10^4$ and should be achievable with a heat load of only 130 W. This is an even more optimistic number than that obtained earlier based on experimental conditions reported by Wu (1991). For comparison, the refrigeration available at Brookhaven is much larger: about 26 kW at 4.2 K. It is noteworthy that the large cell would take about 60 000 l of equivalent liquid at 4.2 K to fill. Once built, such a cell provides a base for a rich variety of ultra-high Re experiments, such as towed or oscillating grid experiments, turbulent bursts, or drag and lift experiments performed by towing bodies of various shapes (Donnelly 1994).

3. Flow ranges attainable with helium and measurement tools

Helium is not only the fluid of lowest viscosity (see figure 2); it also allows one to reach a number of remarkable extremes in various ways which is documented by numbers given in table 3. The superfluid component of helium II can flow in channels larger than the so-called

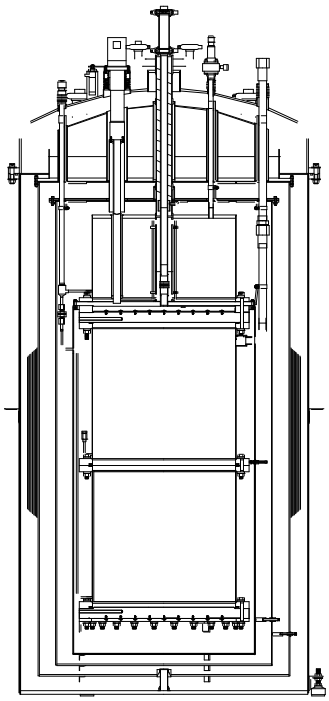

Figure 4. Drawing of the University of Oregon 1 m convection cell. The bottom plate can be moved to change the aspect ratio of the cell. This device is designed to reach Rayleigh numbers of order 10^{16}.

Table 3. Scales of observable flows reachable with helium.

	Smallest	Largest
Rayleigh	(Pure conduction)	$>10^{20}$
Channel size	10 Å	125 cm
Flow velocities	10^{-2} cm s^{-1}	200 m s^{-1}
Reynolds	10^{-3}	10^{9}
Vorticities	10^{-3} Hz	10^{5} Hz

'healing length' (usually a few ångströms except near the lambda transition). The normal fluid can flow when channels are of the order of a few microns or larger. The healing length is essentially the distance over which helium's quantum mechanical wave function goes from its bulk value to zero at the boundary (see, e.g., section 4.4 of Donnelly 1991b). The largest channels likely to be used are probably limited by available helium supplies and refrigeration. Donnelly (1991a) has discussed a liquid helium flow tunnel with up to a 125 cm test section. Very slow velocities have been studied in various flow experiments over the years, while the velocity of sound in helium I would perhaps limit the highest velocities likely to be used in turbulence research.

Reynolds numbers, of course, depend on the characteristic length used to define them. For submarines and ships the length is used to define the Reynolds number, and these can reach values of the order of 4×10^9. As we shall see, even such Reynolds numbers can be matched by the flow of liquid helium on models. Whatever the details are, helium appears as a very

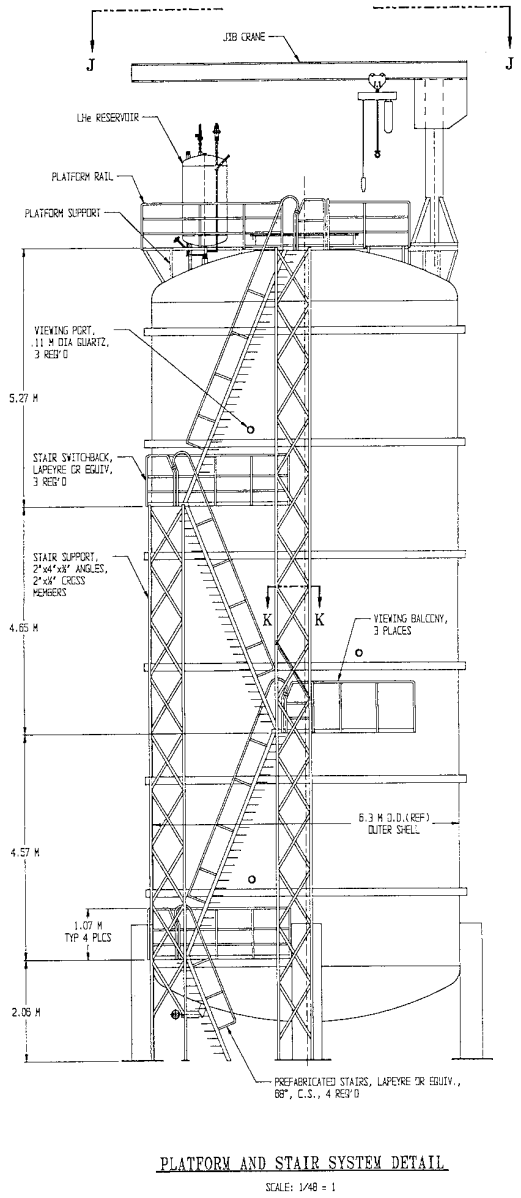

Figure 5. Drawing of the proposed 10 m cell to be placed at Brookhaven National Laboratory designed to reach Rayleigh numbers approaching 10^{20} (after Donnelly 1994).

versatile and useful working substance in fluid mechanics.

A number of suitable instruments are needed to probe such a vast variety of helium flows. In the following we briefly summarize the present state of instrumentation and outline the tasks which lie ahead.

If one wants to measure the average flow velocity in a channel there are a number of methods available. These have been reviewed for cryogenic engineering use in helium II by

Van Sciver *et al* (1991). Methods include turbine flowmeters, venturis, fluidic flowmeters (measuring vortex shedding), acoustic transit time flowmeters and flowmeters based on propagation of temperature or pressure pulses. These methods are applicable to experiments where there is a mean flow velocity, and not to counterflow experiments. Two examples of acoustic flowmeters are given by Swanson and Donnelly (1998).

Temperature gradient and absolute temperature measurements have been developed to a fine art for liquid helium studies. High resolution thermometers developed by Lipa and others now reach sub-nanokelvin resolution. An overview of such technology is given by Lipa (1998).

As we discuss later in this paper, the temperature sensitivity and spatial resolution of thermometers and bolometers is not sufficient to probe the high Re cryogenic helium flows. One has to have micron and even sub-micron size sensors possessing fast time response to be able to probe the very fine scales present in the turbulent flow. Chanal *et al* (1997) recently reported a micron-scale cryogenic thermometer ($1.5 \times 1.5 \times 0.5\ \mu\mathrm{m}^3$) with a response time shorter than 1 μs suitable for high Re turbulence measurements.

A micron-size hot wire anemometer operating at cryogenic temperatures very sensitive to the velocity of a gaseous ^{4}He flow has been developed by Castaing *et al* (1992) and it has since been successfully used to detect various kinds of the turbulent quantities in cryogenic helium flows. Tabeling *et al* (1996) measured probability density functions of the longitudinal velocity increments, skewness and flatness (see, e.g., Monin and Yaglom 1975) for a highly turbulent flow ($150 < Re_\lambda < 5040$) between counterrotating discs in cryogenic helium gas.

To measure lift and drag, it seems to be best to develop magnetic suspension and balance systems. These devices are discussed in depth in several articles by various authors in a book edited by Donnelly (1991a). When operating at helium temperatures, superconducting devices are possible, and the conventional magnets used for many existing systems can be replaced by superconducting magnets. These systems can not only measure lift and drag on a suspended body, they can be used to execute sophisticated manoeuvres at the same time. This reflects their early use for aerodynamical purposes.

There are a number of reasons to use superfluid helium in hydrodynamic experiments, which we shall discuss below. But one reason seldom appreciated is the saving of refrigeration. The kinematic viscosity of liquid helium at 4.2 K is 2.6×10^{-4} cm^2 s^{-1} and it falls steadily with temperature reaching 9×10^{-5} cm^2 s^{-1} at 1.75 K after which it begins to rise again. This represents a factor of 2.89, and since pipe flow, for example, depends on the cube of the kinematic viscosity, going from 4.2 K to 1.75 K takes 24 times less refrigeration. Another advantage is the great ease of stable temperature control. Microdegree stability is routine in small cryostats.

Helium II appears to be a mixture of a superfluid component, which has no viscosity or entropy and a normal component which exhibits viscosity and carries the entire heat content of the fluid. This simplified picture is reflected by the Landau two fluid equations of motion, which have been studied for many years. One dramatic outcome of these equations is the prediction of second sound, a wave described by temperature fluctuations rather than density fluctuations as in ordinary or first sound. A fairly detailed account of equations of motion, quantized vortices, mutual friction and second sound are given in the companion article by Donnelly (1999).

There is one very specific additional tool that can be used to probe the flow of liquid helium. Ion measurements have been carried out for many years in liquid helium. Originally the aim was to study the mobility of the ions and hence to deduce their structure and their interactions with the fluid. When the quantized vortex rings were discovered, ions were the means of deducing their dynamics. Ions have also been used in various ways in hydrodynamics,

including turbulent flows (Donnelly 1991b).

Since ions are trapped on the cores of quantized vortices in helium II, they could, in principle, be used to measure rms vorticity (Milliken *et al* 1982). However, various complications arise when the ions are trapped, as they can move along the cores of the vortices. At the present state of development, ions can locate vorticity spatially in a turbulent flow, but cannot easily determine the magnitude. Interesting experiments using the ion technique to detect the superfluid grid generating turbulence at very low temperature are in progress in Lancaster (Dodd *et al* 1999).

4. High Reynolds number pipe flow

Until recently the highest Reynolds number reported for pipe flow was the experimental work of Nikuradse (see Schlichting 1979, chapter XX), extending to about 3×10^6. Zagarola and Smits (1998), using the Princeton SuperPipe, extended our knowledge of pipe flow by reaching a Reynolds number of 3.5×10^7 (for details, see Zagarola 1996, Zagarola and Smits 1998).

Liquid helium can extend even this range. However, as discussed by Swanson and Donnelly (1998), there is still a great deal of work to be done on cryogenic instrumentation before the full potential of helium measurements can be realized. In particular, as noted by Barenghi *et al* (1995) the attainment of ultra-high Reynolds number by any means is accompanied by a decrease in the size of the smallest eddies, which could reach scales below 100 Å.

Turbulent flow of a conventional fluid of density ρ and average flow velocity U in a smooth pipe of diameter D free from end effects has a dynamic pressure

$$q = \tfrac{1}{2}\rho U^2 \tag{8}$$

and Reynolds number

$$Re = UD/\nu. \tag{9}$$

The pressure drop over a length of pipe L is

$$\Delta P = \lambda \frac{L}{D} q = \frac{1}{2}\lambda Re^2 \left(\frac{L}{D^3}\right)\rho\nu^2 \tag{10}$$

where the friction factor λ is given implicitly by Prandtl's relationship

$$\frac{1}{\sqrt{\lambda}} = 1.889 \log(Re\sqrt{\lambda}) - 0.3577. \tag{11}$$

The volume flow rate is

$$Q = \pi D^2 U/4 \tag{12}$$

and the pumping power is

$$\text{power} = Q\Delta P = \frac{\pi}{8}\lambda Re^3 \left(\frac{L}{D^2}\right)\rho\nu^3 \tag{13}$$

which shows that it varies as the cube of the Reynolds number and of the kinematic viscosity, and accounts for the difficulty of obtaining high Reynolds numbers in the laboratory.

We review the usefulness of superfluid helium II for generating ultra-high Re flow later, but for this particular application the possible limitations are as follows. The highest velocity one could use in a flow with helium II is the velocity of second sound ($\sim$20 m s^{-1} but temperature dependent, going to zero at the lambda transition). If the velocity of second sound is exceeded, second sound shock phenomena will occur. The limitation in helium I is far less confining:

one could presumably go up to the velocity of sound ($\sim$200 m s^{-1}) before encountering shock phenomena.

We show in table 4 some typical design features for a flow circuit that could be run in an academic laboratory, and a flow circuit at Brookhaven using the full capacity of the refrigerator.

Table 4. Examples of pipe flow experiments for an academic laboratory and at BNL.

	Academic laboratory		BNL	
	2.2 K	1.65 K	2.2 K	1.65 K
Tube diameter (cm)	2	2	30	30
Length of test section (cm)	200	200	3000	3000
Reynolds number	1×10^7	2×10^7	2×10^8	4.5×10^8
Friction factor	8.4×10^{-3}	7.65×10^{-3}	5.77×10^{-3}	5.27×10^{-3}
Kinematic viscosity (cm^2 s^{-1})	1.86×10^{-4}	9.16×10^{-5}	1.86×10^{-4}	9.16×10^{-5}
Velocity (cm s^{-1})	931	916	1.24×10^3	1.37×10^3
Total pressure drop (Pa)	7.41×10^3	6.64×10^3	9.99×10^3	1.14×10^4
Assumed pump efficiency	0.5	0.5	0.5	0.5
Total power required (W)	43.3	38.2	17 600	22 250

At Oregon we continue to develop the experiments on a much smaller scale pipe flow apparatus than is shown in table 4. An earlier version using a centrifugal pump is described by Swanson and Donnelly (1998). We are presently working with a new bellows driven pipe flow experiment. Using an electropolished tube of diameter 5 mm connected to the computer controlled bellows systems we generate flows up to Re about 3×10^6 in a laboratory size cryostat. We basically confirm results of Van Sciver (1991) in that the drag deduced from helium II pipe flow appears to be almost classical. This statement is based on the measurements of the pressure drop using a capacitance manometer consisting of a light diaphragm near a fixed electrode as a capacitance transducer (Swanson and Donnelly 1998). The sensitivity has been made extremely high by means of bridges, and can easily detect sub-ångström movements of the diaphragm. A typical resolution is 1 part in 10^8 of the capacitance under study.

5. Tow tanks using liquid helium

Liquid helium has properties that vary rapidly with temperature, especially in helium II. In this section we shall see that these properties can be used to model the motion of ships or waves on a free surface in ways not possible with water. In modelling surface ships we need above all to watch the Froude number

$$Fr = U/\sqrt{gL} \tag{14}$$

where L is the length of the vessel. The Froude number characterizes resistance by wave generation. Suppose we define the scale ratio λ as

$$\lambda = L_w/L_h \tag{15}$$

and adopt the subscript w to denote full scale in water and subscript h for a laboratory model. If we require $Fr_w = Fr_h$, then

$$U_h/U_w = (L_h/L_w)^{1/2} = \lambda^{-1/2}. \tag{16}$$

There are, however, other scaling parameters at a free surface. For example, the Weber number

$$We = \rho U^2 L/\sigma \tag{17}$$

Table 5. Modelling motions on the air/water surface in the laboratory.

Test fluid	α	β	γ
Water	1.23×10^{-3}	1	1
Liquid helium 1.53 K	1.23×10^{-3}	121	15.3

where σ is the surface tension, which governs any surface tension effects, the Reynolds number

$$Re = UL/\nu \tag{18}$$

which governs turbulence effects and finally the ratio α of the liquid density to density of the gas above it. The parameter α and the ratios

$$\frac{Re_h}{Re_w} = \frac{U_h}{U_w}\frac{L_h}{L_w}\frac{\nu_w}{\nu_h} = \frac{\nu_w}{\nu_h}\frac{1}{\lambda^{3/2}} = \frac{\beta}{\lambda^{3/2}} \tag{19}$$

$$\frac{We_h}{We_w} = \frac{\rho_h}{\rho_w}\frac{\sigma_w}{\sigma_h}\frac{1}{\lambda^2} = \frac{\gamma}{\lambda^2} \tag{20}$$

where

$$\beta = \nu_w/\nu_h \qquad \gamma = \rho_h\sigma_w/\rho_W\sigma_h \tag{21}$$

define the temperature dependent material parameters which must be computed for every desired set of operating conditions. One example is given in table 5. From table 5 and the equations above one can see that if we test in water where $\beta = \gamma = 1$ we can match Froude numbers by using (16), but now (19) shows that the Reynolds number is too small by a factor $\lambda^{3/2}$ and (20) shows that the Weber number is too small by a factor λ^2.

To illustrate the situation in current use, let us consider the motion of a surface ship 200 m long, 20 m in diameter, moving at 32 knots (16.5 m s^{-1}). Let us assume the water temperature is 15 °C where the kinematic viscosity is 1.141×10^{-2} cm^2 s^{-1}. The surface tension depends on contaminants and can easily range over a factor of two from 35 to 70 dyne cm^{-1}. We shall take the value for contaminated water as more appropriate for the illustration at hand. If we take $\lambda = 25$ then we have a model 8 m long in a water tow tank and the Froude number (0.373) will be matched (in any fluid) if the model is towed at 3.30 m s^{-1}. However, under these conditions the Reynolds number of the model is 2.31×10^7 compared to the full-scale Reynolds number of 2.89×10^9, that is, the Reynolds number for the model is a factor of $\lambda^{3/2} = 125$ too small. Similarly the Weber number of the ship is 1.56×10^9 and that of the model is 2.49×10^6, a factor of $\lambda^2 = 625$ too small. The water/air density ratio is, of course, correct.

Suppose we consider using a liquid helium tow tank. Consider the tank as a cylinder of radius r and length L_T which is half full (see figure 6). To find the right parameter space, let us first fix the density ratio to be the same as water and air. This leads to an operating temperature of $T = 1.53$ K. If we use (19) to require that both the Froude number and the Reynolds number match then $\lambda^{3/2} = \beta$, or $\lambda = 24.5$ from table 5. We see that at 1.53 K we can match the density ratio, Froude number and Reynolds number, but the Weber number of liquid helium is a factor of 39 too small. This is still a vast improvement over water, however, for which the Weber number is a factor of 600 times too small.

Note that the matching with liquid helium involves picking the scaling ratio λ from the material parameter β, then picking the tow velocity by (16).

The volume of liquid helium to fill this tow tank depends on the length L_T of the tank which sets the desired run time. For $r = 4$ m the volume is

$$V = \tfrac{1}{2}\pi r^2 L = 25.1 L_T \text{ m}^3. \tag{22}$$

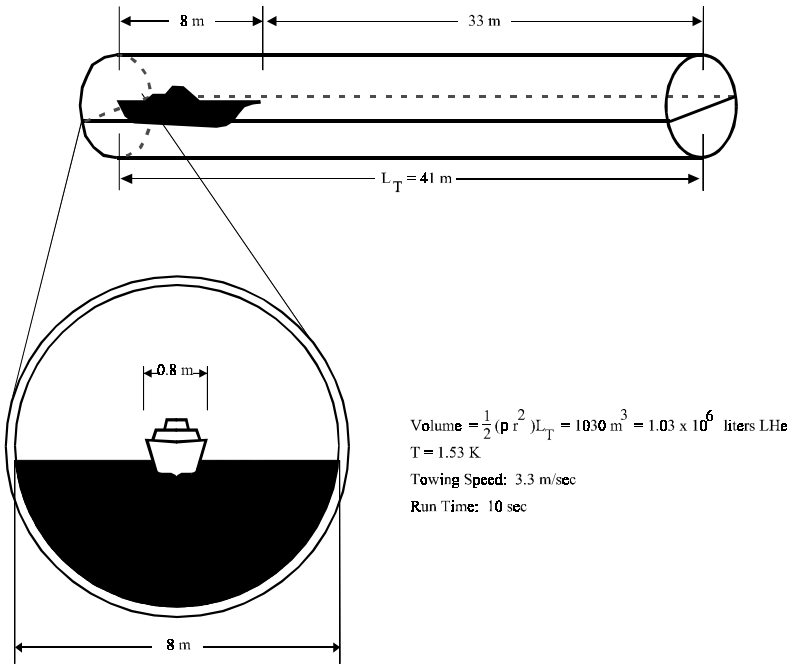

Figure 6. Sketch of a liquid helium tow tank, which is capable of matching more than one parameter at a time, such as Froude number and Reynolds number.

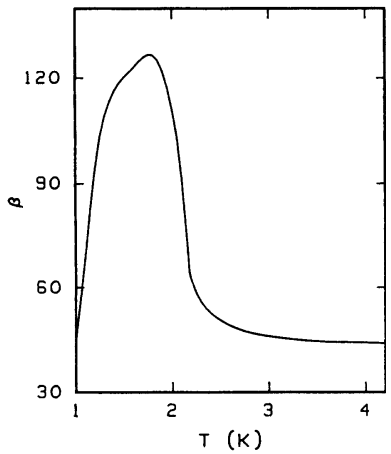

Figure 7. Variation of the parameter β with temperature. The largest values of β and hence of scale parameter λ occur at about 1.75 K if the desire is to match the Reynolds number exactly.

For 10 s of run time at 3.3 m s^{-1}, $L_T = 41$ m and $V = 1.03 \times 10^3$ $m^3 = 1.03 \times 10^6$ l of liquid helium.

We could choose instead, for example, to match the density ratio, Froude number and Weber number. Then $\lambda^2 = \gamma$ and $\lambda = 3.91$. Now the Reynolds number is 15.7 times too large.

Plots of the dimensionless material parameters β and γ as functions of temperature are shown in figures 7 and 8.

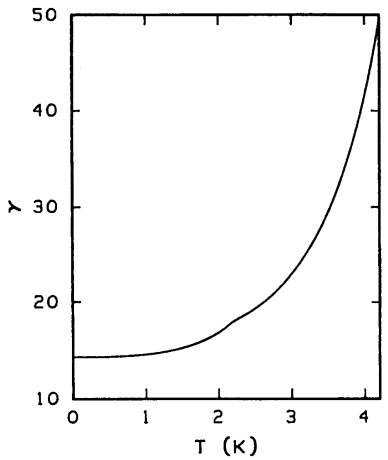

Figure 8. Variation of the parameter γ with temperature. The largest values of γ occur at higher temperatures, giving the largest values of λ if the desire is to match the Weber number exactly.

6. Flow tunnels using liquid helium

Flow tunnels using liquid helium were discussed in chapter 1 of *High Reynolds Number Flows Using Liquid and Gaseous Helium* (Donnelly 1991a). A conceptual design was used as shown in figure 9.

We have used the flow loss design information in the 1966 book by Pope and Harper on low speed wind tunnels to arrive at a conceptual design for a flow facility that could be operated with modest refrigeration requirements. We took as a requirement for such a design that the facility could be built in a conventional low temperature laboratory without major structural changes. At the same time, the capabilities of the facility must be exciting enough to guarantee its usefulness beyond the design and development stage. It is not difficult to see that adopting a relatively small scale for the flow is not difficult. On the other hand, the losses in the flow go as the cube of the flow velocity, and therefore the design needs to be developed around the refrigeration requirement at liquid helium temperatures. We have somewhat arbitrarily chosen a round figure of 100 watts at 1.6 K as the maximum continuous cooling power to be expected to be available without large scale facilities.

The next major quantity to fix is the total volume of liquid helium needed for the working fluid, including dead space in the cryostat. We take the view that a maximum of perhaps 15 000 l would be appropriate to an academic environment—anything larger would be beyond the capability of laboratory liquefiers to maintain. Within these limits it is not difficult to conclude that a maximum jet diameter of 30 cm would be feasible, with 20 cm perhaps the lower limit of usable test sections given the constraints on building models. We show in table 6 operating characteristics for a 30 cm test section. We have taken cross sections as square. To give an idea of performance with models, we have quoted data for drag on a sphere. Here, briefly, is the way the calculations proceed.

The basic configuration of figure 9 for the tunnel was assumed. The physical dimensions were all expressed as multiples of the cross-sectional dimension of the test section. Thus this

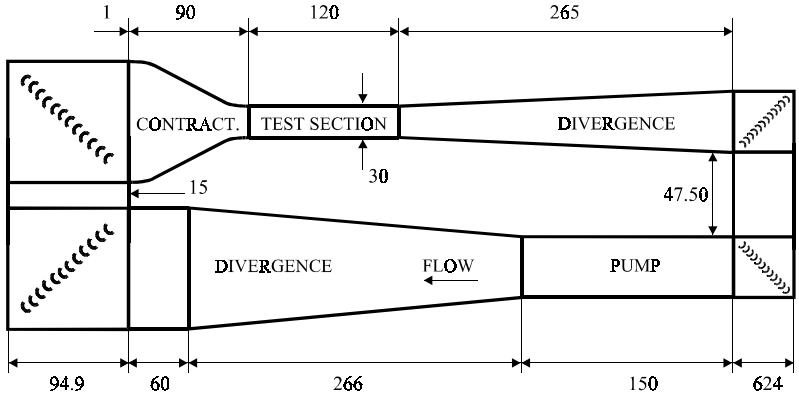

Figure 9. Flow circuit used for low speed tunnel calculations. The dimensions are in centimetres and the example is for a 30 cm test section.

Table 6. Operation of a 30 cm tunnel in helium II: $T = 1.6$ K, $\nu = 9.09 \times 10^{-5}$ cm^2 s^{-1}.

Size of test section (cm)	30
Unit Reynolds number (cm^{-1})	4×10^6
Mach number	0.015
Flow velocity (cm s^{-1})	362
Dynamic head (lb ft^{-1})	19.8
Flow volume (l s^{-1})	256
Shaft power (hp)	0.13
Cooling power required (W)	100
Total power for tunnel (hp)	167
Total liquid helium (l)	17 000
Sphere diameter (cm)	10.7
Drag coefficient	0.65
Sphere Reynolds number	4.26×10^7

cross-sectional dimension together with a desired flow rate (Reynolds number) and temperature became the principal design parameters.

Pressure losses of the individual tunnel components are, in general, a function of the local dynamic pressure q;

$$q = \tfrac{1}{2}\rho U^2 \tag{23}$$

where U is the local flow velocity. Local losses in a particular component were expressed as a product of the local dynamic pressure multiplied by a non-dimensional 'loss coefficient' K which depended only on the dimensions of the component, and local Reynolds number (defined below):

$$\Delta P = \tfrac{1}{2}\rho U^2 K. \tag{24}$$

These loss coefficients have been measured for a wide variety of tunnel configurations and dimensions, the results being expressed in a series of empirical relations of which those in Pope and Harper are a typical (if somewhat conservative) example. The relations in Pope and Harper are generally functionally dependent on such variables as local dimensions of the component, and local Reynolds number:

$$Re = UD/\nu \tag{25}$$

Table 7. Operation of a 125 cm tunnel in helium II: $T = 1.6$ K, $\nu = 9.09 \times 10^{-5}$ cm^2 s^{-1}.

Size of test section (cm)	125
Unit Reynolds number (cm^{-1})	3.9×10^6
Mach number	0.015
Flow velocity (cm s^{-1})	357
Dynamic head (lb ft^{-1})	19.3
Flow volume (l s^{-1})	4377
Shaft power (hp)	1.31
Cooling power required (W)	1000
Total power for tunnel (hp)	1630
Total liquid helium (l)	1.2×10^6
Submarine length (cm)	446
Submarine diameter (cm)	44.6
Drag coefficient	0.10
Submarine Reynolds number	1.75×10^9

where D is the local cross-sectional diameter, and ν is the local kinematic viscosity.

Using conservation of mass, we were then able to reference these local loss coefficients back to the dynamic pressure in the test section. Having thus calculated the loss coefficients (properly referenced back to the test section) for a given configuration and set of design parameters, we added them up to arrive at a total loss coefficient K_{0total}. This in turn by the cross-sectional area and velocity (in the test section) gives the total power consumption required to overcome pressure losses and keep the fluid moving:

$$\text{power} = \Delta P U A = \tfrac{1}{2}\rho U^2 K_{0total} U A = \tfrac{1}{2}\rho U^3 A K_{0total}. \tag{26}$$

This however assumes a perfectly efficient pump which is unrealistic. The final expression for the power necessary to drive the tunnel is thus

$$\text{power} = \frac{1}{2\eta}\rho U^3 A K_{0total} \tag{27}$$

where η is the pump efficiency. We have assumed an efficiency of 50% for the numbers in tables 6 and 7. Note that the unit Reynolds number is the Reynolds number for the entire test section divided by the width in cm.

If we take the most conservative approach, that is to operate in helium I, we still have enormous advantages over water tunnels. For example, supporting the model with a superconducting magnetic suspension system is the *easiest* alternative here. We are well below the transition temperature for many superconductors, and the advantages can be easily and naturally obtained. Moreover, the sensitivity of such superconducting devices as SQUIDs will automatically be available, extending the power of superconducting technology to wind tunnel testing.

Another advantage of using liquid helium is the operation of the tunnel in transient mode. The limiting parameter in the design is the refrigeration available for continuous operation. However, the properties of liquid helium I such as enthalpy and kinematic viscosity do not vary terribly fast with temperature and it is possible to accelerate the pump, allowing the liquid to warm up in the process. Given that the flow circuit will likely be surrounded by a cylindrical dewar, the total volume of the liquid has a great deal of enthalpy. More details are given in Donnelly (1991a) together with comments on using a fountain effect pump instead of an axial flow pump.

Cavitation needs to be considered as well. The cavitation number is defined as

$$Ca = \frac{P - P_v}{1/2\rho U^2} \tag{28}$$

and is the ratio of the difference between the operating pressure and the vapour pressure to the dynamic head. The larger the cavitation number the less likely it is that the fluid will cavitate. In acoustical measurements one tries to avoid cavitation in the flow so large cavitation numbers are desirable.

In helium the difference between pressure and vapour pressure is easily controllable by pressurizing the liquid at a given temperature. Indeed, we have been experimenting with a small pipe flow loop. We do observe cavitation in the pump at high speeds, but a modest increase in pressure (a few psi) is enough to suppress it.

7. Grid generated turbulence experiments in cryogenic helium

Studies of nearly homogeneous and isotropic turbulence produced by grids are of primary importance in the fluid dynamics (see, e.g., Hinze 1975). Experiments are usually performed in wind tunnels that study grid generated turbulence as it decays downstream. Other investigations involve measurements of decaying turbulence created by an oscillating grid in water (De Silva and Fernando 1994). A novel technique where turbulence is created by towing a grid through a stationary sample of helium II was first reported by Smith *et al* (1993); this method was recently also used in water (van Doorn *et al* 1999). Using cryogenic helium as a working fluid can substantially push the attainable limits for this kind of experiment and in the following we outline the recent progress in this direction.

8. Cryogenic helium gas wind tunnel

The enormous advantage of using critical helium gas as a working fluid in a classical wind tunnel can be illustrated using the following example. Let us describe the well known design of the air wind tunnel of Comte-Bellot and Corrsin (1966, 1971). The wind tunnel represents a closed circuit with a 10 m long test section of a 1.0 m $\times$ 1.3 m cross-section. A special feature of the tunnel was a slight secondary contraction that greatly improved homogeneity of the flow. A biplane, square rod grid having typically a mesh size of 5.08 cm and a solidity of 0.34 was used to generate the turbulence. The mean speed of the air past the grid was $U_0 = 10$ m s^{-1}, which corresponds to a mesh Reynolds number of $U_0 M/\nu = 34\,000$. The measured streamwise u_1^2 and transverse u_2^2, u_3^2 velocity components remained nearly equal to each other as they decayed downstream. The turbulence data were collected using the hot wire anemometers. Let us point out that the turbulent data obtained using this wind tunnel are even today regarded as a very accurate and valuable experimental database in decaying grid generated turbulence. This is true despite the fact that the Reynolds number based on the Taylor microscale (see, e.g., Monin and Yaglom 1975) measured about 50 meshes downstream from the grid (where the turbulence can be considered as fully developed) reached only of the order of 100.

We can compare these parameters with the expected performance of a cryogenic helium gas wind tunnel of the size of a conventional laboratory cryostat. The design is based on the test section of only 6×6 cm^{-2} cross section with a grid of the mesh size $M = 0.6$ cm, assuming a measuring probe 50 meshes downstream. Changing the temperature 5 K $< T <$ 78 K and pressure 1 bar $< P <$ 4 bar, assuming the mean velocity is between 2 cm s^{-1} and 2 m s^{-1}, a very broad range of Reynolds numbers based on the Taylor microscale of about

$30 < Re_\lambda < 8000$ can be achieved in a single experiment. Obtaining the turbulent data spanning such an impressive range would be an important step forward towards understanding the physics of grid generated turbulence.

However, generating such a flow is only one aspect of the problem, as one should be also able to probe such flow and measure the relevant turbulent quantities, such as the time dependence of the turbulent velocity. It is desirable to probe the turbulence down to a smallest turbulent scale present in the flow, i.e., the Kolmogorov microscale. This is a challenging problem: the Kolmogorov microscale can become as low as 10^{-7} m. A separate project to develop small hot wire anemometers based on the sputtering of AuGe alloy on thin fibres is already in progress in Oregon. The design, although slightly modified to suit the needs of this application, is based on the anemometer developed earlier by Castaing *et al* (1992). Once completed, the Oregon open flow cryogenic helium wind tunnel should provide an important experimental base for experimental studies of the grid generated turbulence.

9. Towed and oscillating grid experiments in He II

A technique where turbulence is created by towing or oscillating a grid through a stationary sample of helium II and probed by second sound attenuation has been used in Oregon for several years and was first reported by Smith (1992), Smith *et al* (1993) and Stalp *et al* (1999). These experiments are discussed in the companion article by Donnelly in the present issue. The somewhat surprising conclusion is that the decay of turbulence behind a towed grid in helium II can be described essentially classically, although the underlying physics of decaying superfluid turbulence needs special consideration. It is evident that the towed grid in helium II can further our understanding of classical turbulence.

10. Conclusions

We have tried to summarize the reasons why helium is the most likely candidate to achieve controlled ultra-high Reynolds and Rayleigh number flows. Work is now in progress in a number of laboratories to make the possibilities become realities. We hope this paper might stimulate other laboratories to join in this research.

Acknowledgments

All the progress in studying and using the cryogenic helium flows would not have been possible without the knowledge and experience that accumulated during several decades of investigations and development of low temperature physics. We are happy to acknowledge the tremendous contribution and influence of Joe Vinen to this field, starting from his pioneering work on superfluid helium (as described in the paper by Donnelly in this issue) up to recent work on similarities and differences between classical and superfluid turbulence. One of us (LS) had the good fortune to work with Vinen in Birmingham, UK, from 1990 to 1997 and would like to use this opportunity to thank Joe for support, patience, friendship and growth as a physicist under his leadership.

Our research on this subject is supported by the National Science Foundation, grant DMR-95-29609.

References

Ahlers G 1972 Convective heat transport between horizontal parallel plates *Bull. Am. Phys. Soc.* **17** 59–60

——1974 Low temperature studies of the Rayleigh–Benard instability and turbulence *Phys. Rev. Lett.* **33** 1185

Ahlers G and Graebner J E 1972 Time dependence in convective heat transport between horizontal parallel plates *Bull. Am. Phys. Soc.* **17** 61

Arp V and McCarty R D 1998 *Oregon Report on the Properties of Critical Helium Gas* Cryodata Inc.

Ashkenazi S 1997 Turbulent convection in the vicinity of the gas–liquid critical point *PhD Thesis* Weizmann Institute of Science

Barenghi C F, Swanson C J and Donnelly R J 1995 Emerging issues in helium turbulence *J. Low Temp. Phys.* **100** 1–29

Belmonte A 1994 Boundary layer measurements in turbulent convection: vertical plumes in a horizontal wind *PhD Thesis* Princeton

Britcher C P 1998 Application of magnetic suspension and balance systems to Ultra-High Reynolds number facilities *Flow at Ultra-High Reynolds and Rayleigh Numbers* ed R J Donnelly and K R Sreenivasan (New York: Springer) pp 81–95

Castaing B, Chabaud B and Hebral B 1992 Hot wire anemometer operating at cryogenic temperatures *Rev. Sci. Instrum.* **63** 4167–73

Castaing B, Gunaratne G, Heslot F, Kadanoff L and Libchaber A 1989 Scaling of hard thermal turbulence in Rayleigh Benard convection *J. Fluid Mech.* **204** 1–29

Chanal O, Baguenard B, Bethoux O and Chabaud B 1997 Micronic-size cryogenic thermometer for turbulence measurements *Rev. Sci. Instrum.* **68** 2442–6

Chandrasekhar S 1961 *Hydrodynamic and Hydromagnetic Stability* (Oxford: Oxford University Press)

Chavanne X, Chilla F, Chabaud B, Castaing B, Chaussy J and Hebral B 1996 *J. Low Temp. Phys.* **104** 109

——1997 *Phys. Rev. Lett.* **79** 3648

Comte-Bellot G and Corrsin S 1996 The use of contraction to improve the isotropy of grid-generated turbulence *J. Fluid Mech.* **25** 657–82

——1971 Simple Eulerian time correlation of full- and narrow-band velocity signals in grid-generated, 'isotropic' turbulence *J. Fluid Mech.* **48** 273–337

De Silva I P D and Fernando H J S 1994 Oscillating grids as a source of nearly isotropic turbulence *Phys. Fluids* **6** 2455–64

Dodd M E, Hendry P C, Lawson N S, McClintock P V E and Williams C D H 1999 Expansion of liquid helium-4 through the lambda transition *J. Low Temp. Phys.* **115** 89–104

Donnelly R J 1991a Liquid and gaseous helium as test fluids *High Reynolds Number Flows Using Liquid and Gaseous Helium* ed R J Donnelly (New York: Springer)

——1991b *Quantized Vortices in Helium II* (Cambridge: Cambridge University Press)

——1994 *Cryogenic Helium Gas Convection Research; a Report to the Department of Energy* University of Oregon

——1999 Cryogenic fluid dynamics *J. Phys.: Condens. Matter* **11** 7783–34

Donnelly R J and Barenghi C F 1998 The observed properties of liquid helium at the saturated vapor pressure *J. Phys. Chem. Ref. Data* **27** 1217–74

Hinze J O 1975 *Turbulence (McGraw-Hill Classic Textbook Reissue Series)* 2nd edn, ed B J Clark (New York: McGraw-Hill)

Kraichnan R H 1962 *Phys. Fluids* **5** 1374

Lipa J A 1998 Cryogenic thermometry for turbulence research; an overview *Flow at Ultra-High Reynolds and Rayleigh Numbers* ed R J Donnelly and K R Sreenivasan (New York: Springer) 179–83

Maddocks J R 1998 The temperature and pressure dependencies of fluid properties: implication for achieving ultra-high Rayleigh and Reynolds numbers *Flow at Ultra-High Reynolds and Rayleigh Numbers: a Status Report* ed R J Donnelly and K R Sreenivasan (New York: Springer) pp 96–117

Malkus W 1963 *Theory and Fundamental Research in Heat Transfer* (Oxford: Pergamon)

McCarty R D 1972 Thermophysical properties of helium-4 from 2 to 1500 K with pressures to 1000 atmospheres, technical note 631 *National Bureau of Standards*

Milliken F P, Schwarz K W and Smith C W 1982 Free decay of superfluid turbulence *Phys. Rev. Lett.* **48** 1204–7

Monin A S and Yaglom A M 1975 *Statistical Fluid Mechanics: Mechanics of Turbulence* vol 2, trans. Scripta Graphica (Cambridge, MA: MIT Press)

Niemela J J and Donnelly R J 1991 *High Reynolds Number Flows Using Liquid and Gaseous Helium* ed R J Donnelly (New York: Springer) pp 243–52

Niemela J J, Skrbek L and Donnelly R J 1999 *Preprint from LT22 Int. Conf. on Low Temp. Phys. (Helsinki, 1999)*

Pippard A B 1998 private communication

Quack H H 1998 European large scale helium refrigeration *Flow at ultra-High Reynolds and Rayleigh Numbers* ed R J Donnelly and K R Sreenivasan (New York: Springer) pp 52–65
Sano M, Wu X Z and Libchaber A 1989 Turbulence in helium gas free convection *Phys. Rev.* A **40** 6421
Schlichting H 1979 *Boundary-Layer Theory* 7th edn (New York: McGraw-Hill)
Shraiman B and Siggia E Heat transport in high-Rayleigh-number convection 1990 *Phys. Rev.* A **42** 3650
Siggia E 1994 High Rayleigh number convection *Annu. Rev. Fluid Mech.* **26** 137–68
Smith M R 1992 Evolution and propogation of turbulence in helium II *PhD Thesis* University of Oregon
Smith M R, Donnelly R J, Goldenfeld N and Vinen W F 1993 Decay of vorticity in homogeneous turbulence *Phys. Rev. Lett.* **71** 2583–6
Stalp S, Skrbek L and Donnelly R 1999 Decay of grid turbulence in a finite channel *Phys. Rev. Lett.* **82** 4831–4
Swanson C and Donnelly R J 1998 Instrument development for high Reynolds number flows in liquid helium *Flow at Ultra-High Reynolds and Rayleigh Numbers* ed R J Donnelly and K R Sreenivasan (New York: Springer) pp 206–22
Tabeling P, Zocchi G, Belin F, Maurer J and Willaime H 1996 Probability density functions, skewness, and flatness in large Reynolds number turbulence *Phys. Rev.* E **53** 1613–21
Threlfall D C 1975 Free convection in low-temperature gaseous helium *J. Fluid Mech.* **67** 17–28
Tritton D J 1988 *Physical Fluid Dynamics* 2nd edn (Oxford)
van Doorn E, White C M and Sreenivasan K R 1999 The decay of grid turbulence in polymer and surfactant solutions *Phys. Fluids* at press
Van Sciver S W 1991 Experimental investigations of He II flows at high Reynolds number *High Reynolds Number Flows Using Liquid and Gaseous Helium* ed R J Donnelly (New York: Springer) pp 223–32
Van Sciver S W, Holmes D S, Huang X and Weisend J G II 1991 Helium II Flowmetering *Cryogenics* **31** 75
Woodcraft A L, Lucas P G, Matley R G and Wong W Y 1998 First images of controlled convection in liquid helium *Flow at Ultra-High Reynolds and Rayleigh Numbers* ed R J Donnelly and K R Sreenivasan (New York: Springer) pp 436–49
Wu X U and Libchaber A 1991 Non-Boussinesq effects in free thermal convection *Phys. Rev.* A **43** 28–33
Wu X Z 1991 Along the road to developed turbulence: free thermal convection in low temperature helium gas *PhD Thesis* University of Chicago
Zagarola M V 1996 Mean-flow scaling of turbulent pipe flow *PhD Thesis* Princeton
Zagarola M V and Smits A J 1998 The mean velocity profile in turbulent pipe flow *Flow at Ultra-High Reynolds and Rayleigh Numbers* ed R Donnelly and K Sreenivasan (New York: Springer) pp 200–5